

# Green Microstructural Visualization of Dry-Pressed Spray-Dried Alumina ( $\text{Al}_2\text{O}_3$ )

Ian P. Maher, Richard A. Haber

Department of Materials Science and Engineering, Rutgers University, Piscataway, NJ, USA

Email: ipa.maher@gmail.com

**How to cite this paper:** Maher, I.P. and Haber, R.A. (2018) Green Microstructural Visualization of Dry-Pressed Spray-Dried Alumina ( $\text{Al}_2\text{O}_3$ ). *Materials Sciences and Applications*, 9, 936-948.

<https://doi.org/10.4236/msa.2018.912067>

**Received:** October 9, 2018

**Accepted:** November 12, 2018

**Published:** November 15, 2018

Copyright © 2018 by authors and Scientific Research Publishing Inc.

This work is licensed under the Creative Commons Attribution-NonCommercial International License (CC BY-NC 4.0).

<http://creativecommons.org/licenses/by-nc/4.0/>



Open Access

## Abstract

Slurry parameters were controlled prior to spray-drying to visualize and govern an understanding of which parameters govern hollow coring and granule morphology during spray-drying. An aqueous alumina using a polyvinyl alcohol binder (PVA) system was analyzed and granules were processed by altering the slurry specific gravity and viscosity value prior to spray-drying. Spray-dried granules were uniaxial dry-pressed at varying moisture contents to show the plasticizing effects of moisture during compaction. A novel characterization method using a field emission electron microscope (FESEM) was implemented to image the green microstructures of the granules and compacted samples. Slurries with a higher specific gravity and viscosity resulted in denser granules with spherical shapes. Viscosity affected the binder segregation during the spray-drying process. Granules stored at higher moisture contents resulted in denser compacts with fewer intergranular pores and cracks along granule boundaries. Using a FESEM resulted in higher resolution for green microstructural characterization.

## Keywords

Spray-Dried Alumina, Uniaxial Dry-Pressing, SEM, Green Microstructural Imaging

## 1. Introduction

Microstructural variability in ceramic green bodies has been a known issue within the ceramic processing world. Dry-pressing of ceramic powders is a widely used process due to its low cost, high production rates, and shape forming abilities. Fine ceramic particles typically achieve high-density parts at lower temperatures and times due to enhanced sintering kinetics. However, fine particles do not flow due to the interparticle attractive forces, which are greater than

the force of gravity. This reason is what hinders die filling uniformity and the green (nonsintered) bulk consistency of the compacted ceramic. To improve the flowability of fine ceramic particles, a granulation technique is desirable. In dry-pressing, agglomerated powders are created in the form of flowable granules. Spray-drying is the most widely used granulation technique for large production of dry-pressed ceramics. A key requirement during the dry-pressing process is a uniform density distribution of primary ceramic granules, without which causes variations in green bulk density. A desired uniform green microstructure shows no remnants of the agglomerated granules and a uniform density distribution. If granule remnants remain, intergranular pores will persist within the microstructure after densification, thus depleting the reliability of the ceramic's properties. Large pores that persist throughout the sintered microstructure can become stress concentrators and cause failures during production. A major challenge in dry-pressing ceramics is processing a flaw free green microstructure that will return a highly reliable sintered ceramic. Different factors in the processing of compacted green body ceramics lead to microstructural variations that are difficult to account for. Characterization and evaluation of the ceramic green microstructure are necessary to form reliable dry-pressed ceramics. The issue is there is an absence of sufficient analytical techniques needed to characterize the microstructure of the green ceramic compacts. This paper will describe a novel characterization method to visualize green ceramics with the use of a field emission scanning electron microscope.

## 2. Background

### 2.1. Liquid Immersion Method (LIM)

In terms of microstructural visualization of green ceramics, a novel technique using an optical microscope was developed by Uematsu *et al.* [1] known as the liquid immersion method (LIM) to visualize the morphology of spray-dried granules. Alumina spray-dried granules were made transparent under an optical microscope by use of an immersion liquid to account for the refractive index of the alumina ceramic, which is  $n = 1.76$  [1]. Methylene iodide ( $n = 1.74$ ) and 2-bromonaphthalene ( $n = 1.64$ ) were the immersion liquids tested since they have a similar refractive index of alumina [1]. The relative refractive indices of these liquids compared to alumina are  $R = 1.01$  for the former and  $1.07$  for the latter [1]. The interior structures of the spray-dried granules were examined to determine if they were solid or hollow [1]-[15]. This method proved to visualize the segregation of PVA binder within the internal structure of the granule. Zhang *et al.* [2] showed the distribution of PVA within the compacted body and how binder rich layers cause detrimental defects prior to sintering. Dry-pressed alumina green bodies were thinned by the use of a grinding sandpaper to less than 0.5 mm in thickness and an immersion liquid was used to visualize the uniformity of the compacted microstructure. Regions of high and low density were then differentiated based on the binder distribution within the granules, and

thus, the compacted green body [1] [5] [6] [7] [9] [11] [16]. It was found that large intergranular pores formed in between the remnant structures of the compacted granules that have PVA rich layers on the surface. These pores persisted and formed detrimental defects within the sintered body. Density gradients also formed within the compacted body. Once the binder rich layers were removed during the sintering process, regions of low density formed along granule boundaries [2] [6] [7] [9] [12] [16]. **Figure 1** shows the liquid immersion method and the binder distribution within granules and a compacted green body before and after binder removal [17].

Uematsu *et al.* [8] coupled infrared microscopy with the liquid immersion method to improve the capability with other ceramics. Silicon nitride, for example, has a refractive index of  $n = 2.05$ , and all available immersion liquids to be used are toxic and unstable, therefore using a longer wavelength light source, such as infrared light, can be helpful for observation [8]. Due to the stronger light source, a thickness of 2 mm of specimens to be observed was achieved as opposed to 0.5 mm with an optical microscope. However, the availability of immersion liquids for most ceramics with high refractive indices is low. This reason, along with thinning the specimens down in thickness and intermediately sintering the specimens to elevated temperatures around  $1000^{\circ}\text{C} - 1100^{\circ}\text{C}$  are the major limitations of this method [3]. The purpose of heating the samples to the above temperatures is to supply enough strength for handling during the characterization process [3]. However, its capabilities used to visualize the binder segregation and internal structures of spray-dried granules and compacted green bodies have been proven valuable in ceramic processing.

## 2.2. Confocal Laser Scanning Microscopy (CLSM)

Confocal laser scanning microscopy (CLSM) is an improved method that uses a fluorescent dye and an immersion liquid within a green compact. Saito *et al.* [18] has stated that this method can show the smallest features of roughly 0.4 microns, which is an improvement from the liquid immersion method. With this method, low density regions were shown to form at granule boundaries after binder burnout [19]. This method has also shown the processing effects of different relative humidity atmospheres on the compaction behavior of spray-dried granules and the resulting green microstructures [18] [19] [20]. Brighter contrast regions show the effect PVA segregation has on the microstructure of the green compact, forming detrimental intergranule porosity. Homogeneous microstructures formed with higher relative humidity percentages resulted in higher strength and reliable ceramics [20]. Tanaka *et al.* [21] investigated the difference between ball milled and agitated ball milled processing in terms of producing spray-dried granules. It was shown that ball milled granules resulted in a higher percentage of agglomerates and aggregates within the granule compared to agitated ball milled. Kato *et al.* [22] investigated the stages of compaction using this method by tapping granules within a die by use of a high refractive index resin and fluo-

rescent dye in an attempt to visualize the behavior of spray-dried granules deforming in the initial stage of compaction at a pressure of 2 MPa. It was found difficult to quantify the deformation process using this method.

The limitations of this method are the same as the liquid immersion method previously discussed. This method resolves heavily on the use of an immersion liquid with a high enough refractive index to characterize the green compacted ceramic. Alumina is heavily investigated due to its easily accessible refractive index for analysis [18]-[23]. Compacted green ceramics must also have a high strength to be thinned to less than 0.2 mm for this method, therefore be heated to temperatures around 700°C - 1000°C [18] [19]. These limitations restrict the capabilities of spatial resolution and, on a larger scale, three-dimensional imaging [18]. **Figure 2** shows the improved resolution with using CLSM to visualize the binder distribution along the granule boundaries within a compacted green body.

### 2.3. Micro X-Ray Computed Tomography (Micro X-Ray CT)

Micro X-ray computed tomography (micro X-ray CT) is a nondestructive characterization tool that has been recently used to visualize the internal structure of materials [17] [24]. Dies *et al.* [25] investigated the moisture effects during

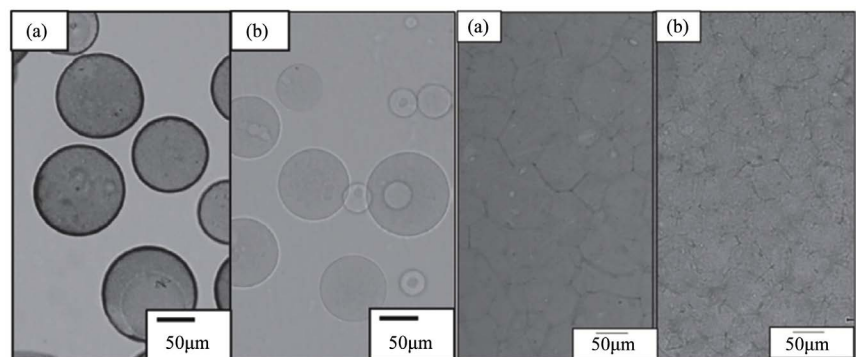


**Figure 1.** (Left) Images taken using LIM showing the PVA binder distribution within spray-dried granules (a) before and (b) after binder burnout from Hondo *et al.* [17]. (Right) Compacted microstructure (a) before and (b) after binder burnout showing intergranular pores and low density regions from Hondo *et al.* [17].

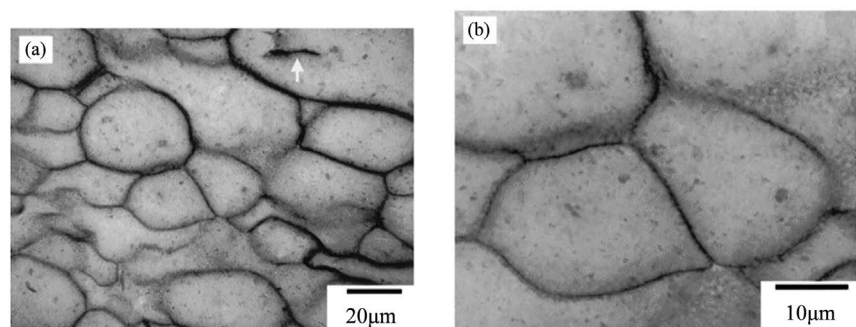


**Figure 2.** Image generated from CLSM showing PVA binder distribution within compacts from Saito *et al.* [19].

compaction with this technique. Spray-dried granules were stored at varying relative humidity levels prior to compaction. Their respective densities were calculated by the final length measurement after compaction. Density distributions throughout the compacted green body were examined. Granules stored under no humidity resulted in a greater uniformity throughout the compacted body when compared to spray-dried granules stored at 98% relative humidity, which resulted in the greatest density but had a greater difference of density variations throughout the microstructure. The most uniform structure resulted from granules stored at a relative humidity level of 60%. A similar study was completed by Cottrino *et al.* [26] where density heterogeneity was highlighted by manipulating the compaction behavior of the spray-dried granules due to varying moisture and binder percentages of the granules prior to compaction.

In micro X-ray CT, large pores and loose packing structures within the ceramic compact are difficult to distinguish due to the similar degrees of X-ray absorbency [27]. Potassium iodide was used as a contrast media by Hondo *et al.* [24] in attempt to account for this issue and is shown in **Figure 3**. Hondo was able to visualize areas of low density regions within green ceramics down to a resolution of one micron and generated a three-dimensional rendering of the characterized ceramic [24]. Hondo went on to evaluate the growth behavior of large pores during sintering with the use of micro X-ray CT and was able to show heterogeneous densification occurs due to large pore growth and nonuniform granule remnant shrinkage [17].

#### 2.4. Field Emission Scanning Electron Microscope (FESEM)

Ku [28] developed a method using Spurr Low Viscosity Kit epoxy to infiltrate ceramic powders within interparticle pores without causing dispersion or breakage. Alazzawi *et al.* [29] has shown this infiltration method can successfully infiltrate green titanium dioxide extrudates for microstructural characterization with the use of a FESEM and charge mitigation techniques for higher resolution microstructural characterization. This method will be the method investigated for this paper.

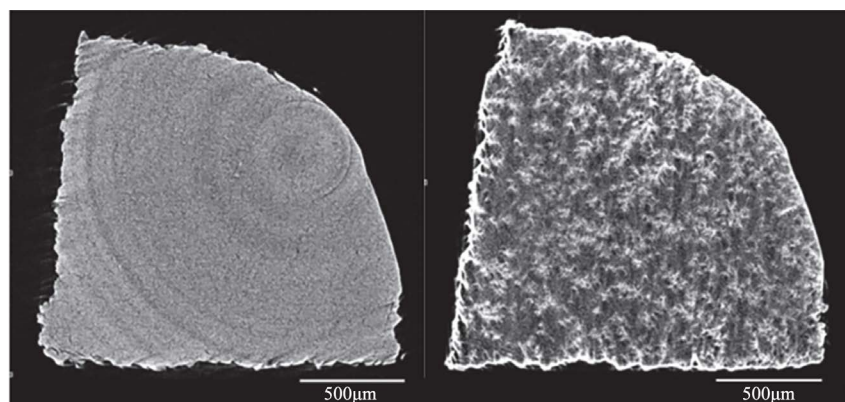


**Figure 3.** X-ray CT generated image (Left) before and (Right) after the use of potassium iodide from Hondo *et al.* [24].

### 3. Experimental Approach

#### 3.1. Granule Morphology Analysis

The alumina powder used in the slurry was A16-SG alumina from Almatris Incorporated (Almatris Inc.—Leetsdale, PA). The binders used in the slurry were polyethylene-glycol (PEG) and polyvinyl-alcohol (PVA). The PEG used was PEG 300 from Acros Organics (Acros Organics—ThermoFisher Scientific, Waltham, MA) and the PVA used was a 20% aqueous solution prepared by SELVOL (SELVOL E 205 PVA) and distributed by Sekisui (Sekisui—Secaucus, NJ). The dispersant used in the slurry was ammonium polyacrylate (Darvan 821A). PVA binder was added at 1.50% based on the solids weight within the slurry [30] [31]. The PEG 300 was kept constant in all slurries at 0.15% based on the solids weight and acted solely as a plasticizer for the binder. Alumina slurries were processed and milled for 24 hours in 500 mL Nalgene bottles and 22 hours in 1 liter alumina jars [30] [31]. The main concern with changing the time was to ensure all slurries had the same milled particle size. More dispersant was added in the final milling hour to drop the viscosity prior to spray-drying [30]. The initial percentage of dispersant added was 0.1% based on the solids weight within the slurry. The viscosities varied from 100 cP, 250 cP, and 400 cP (Brookfield, 20 RPM, and Spindle RV03). The specific gravity of the slurries varied from 1.48 (50 wt%/31 vol.% solids), 1.70 (55 wt%/36 vol.% solids), and 1.80 (60 wt%/41 vol.% solids). The additional percentage of dispersant added within the last hour of milling varied depending on the specific gravity of the slurry and the desired viscosity range. The specific gravity and viscosity of the slurries varied prior to spray-drying in attempt to visualize a relationship between slurry characteristics and the characteristics of the spray-dried granules.

The spray-dryer used for this study was a Niro Atomizer Minor Plant with a co-current fountain nozzle. The slurries were pumped and atomized into the nozzle at a constant speed and atomization pressure. The inlet temperature of the spray-dryer was set to 150°C with the outlet ranging from 60°C - 70°C [5] [6]. The powder was then screened through varied sized sieves to evaluate particle size analysis on the spray-dried granules. The moisture of the spray-dried granules varied from 0.0% - 0.5% moisture based on weight and no further heat treatment was conducted to ensure the mechanical properties of the organic binder were governed. In preparation for image analysis, the granules were heat treated at 150°C with a ramp heat of 10°C per minute. Granules were dwelled for two hours at 150°C and then cooled to room temperature, 25°C, at a rate of 10°C per minute.

Granules were then vacuum infiltrated using a Buehler Cast N' Vac 1000 (Buehler—Lake Bluff, IL) and Spurr Low Viscosity Epoxy Kit prepared by Electron Microscopy Sciences (EMS—Hatfield, PA). This epoxy infiltrates into the submicron pores of the green alumina sample without causing breakage. The infiltrated samples were then polished down to 0.05 μm using a mechanical polisher [28] [29]. For the final step in preparation for characterization, the sam-

ples were ion milled using a Hitachi IM4000 Ion Mill by flat milling the surface of the samples at a voltage of 6 kV for 10 minutes. To address the porous nature of the specimens, techniques were implemented to mitigate the charging effect during SEM characterization. The polished samples were coated in silver paste around every part of the epoxy except for the polished surface of the sample and sputtered with fifteen nanometers of gold. Obtaining images of similar brightness and contrast was attempted for better comparison. This was achieved by using a similar detector, working distance, and brightness and contrast values during the analysis. A Field Emission Scanning Electron Microscope (FESEM) from Zeiss was used during the microstructural analysis (Zeiss—Oberkochen, Germany).

### 3.2. Green Microstructure Analysis

In an attempt to understand the processing effects on microstructural uniformity within a uniaxial dry-pressed compact, moisture was added to specific spray-dried granules to understand what role moisture plays alongside the PVA binder during dry-pressing. It is known that moisture softens the spray-dried granules as a plasticizer and lowers the glass transition temperature ( $T_g$ ) of the organic binder. The yield strength of the granules decreases but the hope is to visualize the microstructure and to account for the formation of intergranular voids and pores.

Spray-dried granules in the size range of 55  $\mu\text{m}$  to 75  $\mu\text{m}$  of the 250 cP (55% Solids) were placed in a humidity cabinet at 95% relative humidity to add moisture to the granules. The moisture percentage was calculated by weight loss using Arizona Instruments Computrak 2000 moisture analyzer by heating up the granules to 115°C for 10 minutes. To ensure the weight loss wasn't being attributed to the loss of the organic binder species, TGA was administered by use of a TA Instruments Q600 by heating up the granules to 700°C at a rate of 3°C per minute in air for 2 hours. It was found that the PVA started to degrade roughly around 125°C. Granules were uniaxially compacted to 100 MPa at moisture percentages of 0.1% (As-Received Spray-Dried) and 3.0%. Compacted green bodies were then vacuum infiltrated, polished, ion milled, and prepared for FESEM microstructural image analysis using the same method described above for the spray-dried granules in the previous subsection.

## 4. Results and Discussion

### 4.1. Granule Morphology Analysis

FESEM images of the spray-dried granules obtained by various slurry parameters are shown below in **Figures 4-8**. Their tap densities are 0.94  $\text{g}/\text{cm}^3$ , 0.95  $\text{g}/\text{cm}^3$ , 1.00  $\text{g}/\text{cm}^3$ , 0.92  $\text{g}/\text{cm}^3$ , and 1.00  $\text{g}/\text{cm}^3$  for 100 cP (55% solids), 250 cP (55% solids), 400 cP (55% solids), 50% Solids (400 cP), 60% Solids (400 cP) respectively. These values are an average of three calculations for the same granule sieve sizes. Tap density values show higher specific gravity and viscosity of the aqueous slurries promote denser granules and less hollow coring. FESEM image analysis

shows the variations in hollow coring for the spray-dried granules and shows proof of the past statement. All FESEM images below are taken using an InLens detector to enhance the contrast difference of the spray-dried granules infiltrated in the epoxy resin. Hollow coring was extensive in the 100 cP (55% solids) granules compared to the rest and showed greater hollow cores in size compared to the others. 400 cP and 60% solids showed some irregular shapes but less frequent hollow coring that were smaller in size compared to the 100 cP and 50% solid granules.

#### 4.2. Green Microstructure Analysis

SEM images of microstructures of the varying moisture percentages are shown below in **Figure 9** and **Figure 10**.

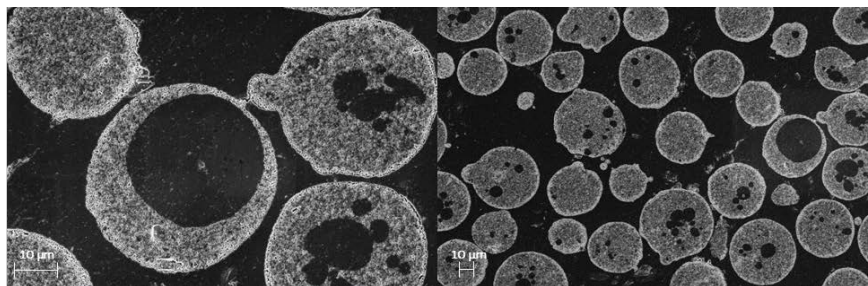


**Figure 4.** FESEM micrographs of 100 cP (55% solid) granules at a sieve size of 55 µm to 75 µm. Hollow core size is very large (almost at the granule wall) when compared to others.

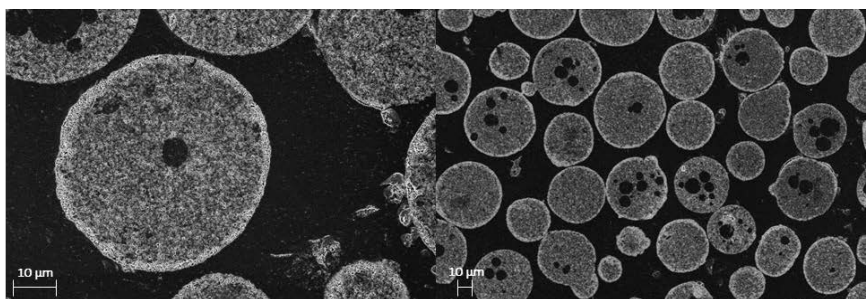


**Figure 5.** FESEM micrographs of 250 cP (55% solid) granules at a sieve size of 55 µm to 75 µm.

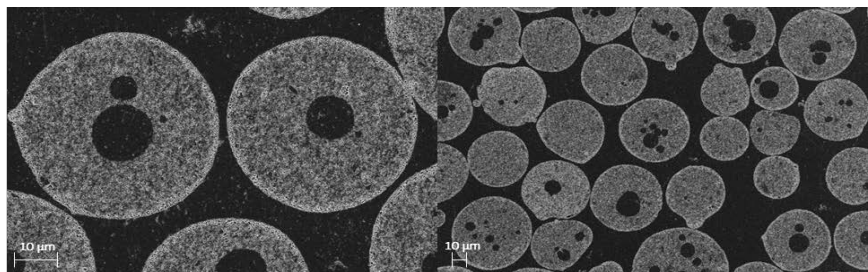


**Figure 6.** FESEM micrographs of 400 cP (55% solid) granules at a sieve size of 55 µm to 75 µm. Irregular shaped granules were more abundant but smaller hollow coring was shown.

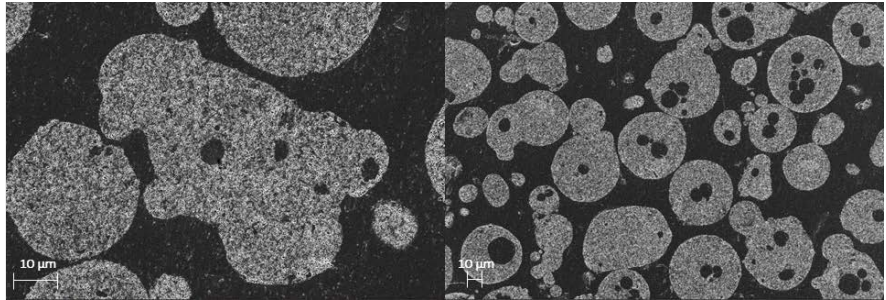


**Figure 7.** FESEM micrographs of 400 cP (50% solid) granules at a sieve size of 55 µm to 75 µm. Irregular shaped granules were more abundant but smaller hollow coring was visualized.

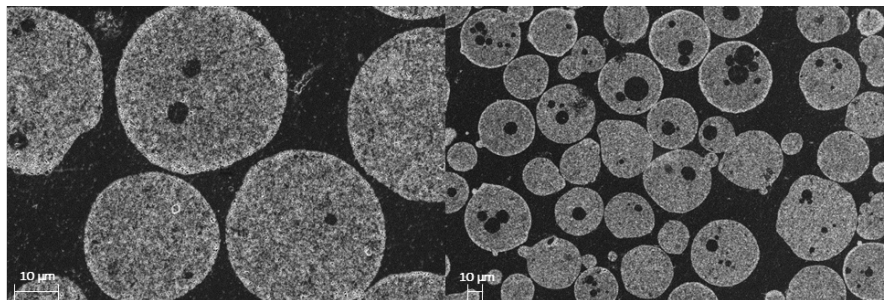


**Figure 8.** FESEM micrographs of 400 cP (60% solid) granules at a sieve size of 55 µm to 75 µm. Denser granules were more abundant but smaller hollow coring was visualized.

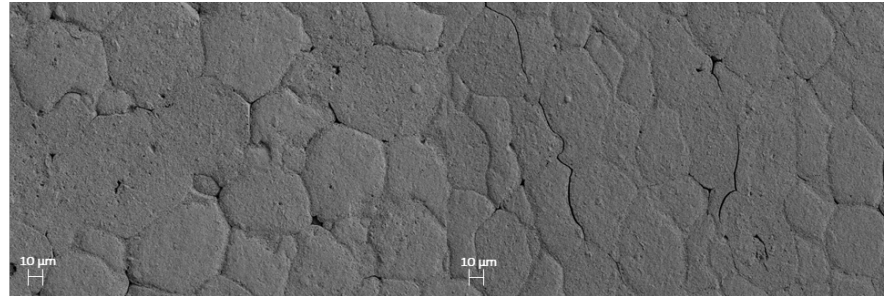


**Figure 9.** FESEM microstructure of a 100 MPa uniaxially compacted green body at dry or 0.1% moisture content.

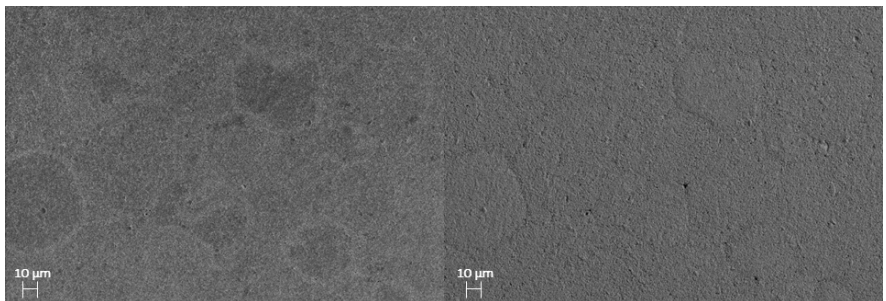


**Figure 10.** FESEM microstructure of a 100 MPa uniaxially compacted green body at 3.0% moisture content. The image on the left was taken with an InLens detector on the Zeiss FESEM and the image on the right is the same region of the green alumina microstructure taken using an SE2 detector.

At 0.1%, the remnants of the granules can still be seen, however at 3.0% moisture, the granule remnants are no longer visible. Less intergranular pores and cracks along low-density regions of the granule boundaries are visible in the compacts pressed with 3.0% moisture. The green densities of the alumina compacts for 3.0% and dry (0.1%) are 56.5% and 56.0% respectively. These densities are geometric densities calculated by the volume of the compact and weight after the compact was heat treated to remove the organic binder. The alumina compacts were heated up to 700°C at a rate of 3°C per minute in air for 2 hours to achieve this calculation. In **Figure 7**, the image on the left was taken with an In-Lens detector on the Zeiss FESEM, to distinguish a contrast difference between the organic binder species of PVA located on the granule boundaries and the alumina ceramic. The image on the right is the same region of the green alumina microstructure taken using an SE2 detector instead, to show the uniformity comparison with the above microstructures at 0.1% moisture in **Figure 9**. During spray-drying, the PVA binder migrates to the surface of the ceramic particles during the evaporation of the water. This creates a segregated layer of organic binder that dictates the knitting of the granules during compaction. If cracks form along the granule boundaries after compaction, low density regions will form along the granule boundaries after the binder removal process. The 3.0% moisture content showed a higher degree of uniformity in the green microstructural FESEM images than the 0.1% or as-received dry granules did. There was a higher degree of intergranular pores and voids along the granule boundaries within the 0.1% microstructure than the 3.0% granules. During binder removal, these large voids and cracks along the granule boundaries create low density regions within the compact and therefore a flawed green microstructure. Visualizing these processing differences prior to dry-pressing ceramic granules will aid in processing more reliable ceramic materials.

## 5. Conclusion

The use of a low viscosity epoxy resin to infiltrate compacted green bodies without breakage or dispersion coupled with a unique polishing and ion milling technique has been proved successful in visualization and green microstructural evaluation of spray-dried granules and compacted green bodies. The conductive materials used to mitigate the charging effects of the porous ceramics are proved to be enough to counter issues that evolve from microscopy characterization of porous materials. This novel technique shows the issues that arise from varying processing parameters of spray-dried granules and compacted green bodies. Hollow coring was visualized to be more abundant in granules that were spray-dried with lower viscosity and specific gravity values. Irregular shaped granules were shown to be more prevalent in granules spray-dried from slurries with a viscosity of 400 cP and 50% solids loading by weight. Adding moisture to the spray-dried granules aids in the removal of intergranular pores and cracks along the granule boundaries, however, the issue that arises becomes the forma-

tion of density gradients that can only be visualized three-dimensionally.

## Acknowledgements

This research was sponsored by the National Science Foundation I/UCRC Award No.1540027. The views and conclusions contained in this document are those of the authors and should not be interpreted as representing the official policies, either expressed or implied, of the National Science Foundation or the US Government. The US Government is authorized to reproduce and distribute reprints for Government purposes notwithstanding any copyright notation herein.

Thank you to everyone who helped with this research: Mustafa K. Alazzawi, Ashley Luster and Satya Sweta Kondapalli (Rutgers University); Leslie Fenwick for the A16 alumina used in this study (Almatis Corporation); Dr. Jay Martin for the SERVOL PVA binder used in this study (St. Gobain).

## Conflicts of Interest

The authors declare no conflicts of interest regarding the publication of this paper.

## References

- [1] Uematsu, K., Kim, J. Y., Miyashita, M., Uchida, N. and Saito, K. (1990) Direct Observation of Internal Structure in Spray-Dried Alumina Granules. *Journal of the American Ceramic Society*, **73**, 2555-2557. <https://doi.org/10.1111/j.1151-2916.1990.tb07635.x>
- [2] Zhang, Y., Uchida, N. and Uematsu, K. (1995) Direct Observation of Non-Uniform Distribution of PVA Binder in Alumina Green Body. *Journal of Materials Science*, **30**, 1357-1360. <https://doi.org/10.1007/BF00356144>
- [3] Uematsu, K. (1996) Immersion Microscopy for Detailed Characterization of Defects in Ceramic Powders and Green Bodies. *Powder Technology*, **88**, 291-298. [https://doi.org/10.1016/S0032-5910\(96\)03133-6](https://doi.org/10.1016/S0032-5910(96)03133-6)
- [4] Zhang, Y., Tang, X., Uchida, N. and Uematsu, K. (1998) Binder Surface Segregation during Spray Drying of Ceramic Slurry. *Journal of Materials Research*, **13**, 1881-1887. <https://doi.org/10.1557/JMR.1998.0267>
- [5] Hotta, T., Nakahira, K., Naito, M., Shinohara, N., Okumiya, M. and Uematsu, K. (1999) Origin of Strength Change in Ceramics Associated with the Alteration of Spray Dryer. *Journal of materials research*, **14**, 2974-2979. <https://doi.org/10.1557/JMR.1999.0398>
- [6] Shinohara, N., Okumiya, M., Hotta, T., Nakahira, K., Naito, M. and Uematsu, K. (1999) Formation Mechanisms of Processing Defects and Their Relevance to the Strength in Alumina Ceramics Made by Powder Compaction Process. *Journal of Materials Science*, **34**, 4271-4277. <https://doi.org/10.1023/A:1004611105281>
- [7] Shinohara, N., Okumiya, M., Hotta, T., Nakahira, K., Naito, M. and Uematsu K. (1999) Seasonal Variation of Microstructure and Sintered Strength of Dry-Pressed Alumina. *Journal of the American Ceramic Society*, **82**, 3441-3446. <https://doi.org/10.1111/j.1151-2916.1999.tb02262.x>
- [8] Uematsu, K., Uchida, N., Kato, Z., Tanaka, S., Hotta, T. and Naito M. (2001) Infra-

- red Microscopy for Examination of Structure in Spray-Dried Granules and Compacts. *Journal of the American Ceramic Society*, **84**, 254-256. <https://doi.org/10.1111/j.1151-2916.2001.tb00646.x>
- [9] Shinohara, N., Katori, S., Okumiya, M., Hotta, T., Nakahira, K., Naito, M., *et al.* (2002) Effect of Heat Treatment of Alumina Granules on the Compaction Behavior and Properties of Green and Sintered Bodies. *Journal of the European Ceramic Society*, **22**, 2841-2848. [https://doi.org/10.1016/S0955-2219\(02\)00059-6](https://doi.org/10.1016/S0955-2219(02)00059-6)
- [10] Saito, Y., Nyumura, J., Zhang, Y., Tanaka, S., Uchida, N. and Uematsu, K. (2002) Kinetics of Property Change Associated with Atmospheric Humidity Changes in Alumina Powder Granules with PVA Binder. *Journal of the European Ceramic Society*, **22**, 2835-2840. [https://doi.org/10.1016/S0955-2219\(02\)00041-9](https://doi.org/10.1016/S0955-2219(02)00041-9)
- [11] Saito, Y., Nyumura, J., Fukai, K., Zhang, Y., Uchida, N. and Uematsu, K. (2002) Moisture Diffusion in Alumina Green Compact Containing Polyvinyl Alcohol Binder. *Journal of the Ceramic Society of Japan*, **110**, 237-242. <https://doi.org/10.2109/jcersj.110.237>
- [12] Tanaka, S., Pin, C.C. and Uematsu, K. (2006) Effect of Organic Binder Segregation on Sintered Strength of DRY-Pressed Alumina. *Journal of the American Ceramic Society*, **89**, 1903-1907. <https://doi.org/10.1111/j.1551-2916.2006.01057.x>
- [13] Tanaka, S., Chia-Pin, C., Kato, Z. and Uematsu, K. (2007) Effect of Internal Binder on Microstructure in Compacts Made from Granules. *Journal of the European Ceramic Society*, **27**, 873-877. <https://doi.org/10.1016/j.jeurceramsoc.2006.04.038>
- [14] Imran, Z.M., Tanaka, S. and Uematsu, K. (2009) Effect of Polyacrylic Acid (PAA) Binder System on Particle Orientation during Dry-Pressing. *Powder Technology*, **196**, 133-138. <https://doi.org/10.1016/j.powtec.2009.07.003>
- [15] Zainuddin, M.I., Tanaka, S., Furushima, R. and Uematsu, K. (2010) Correlation between Slurry Properties and Structures and Properties of Granules. *Journal of the European Ceramic Society*, **30**, 3291-3296. <https://doi.org/10.1016/j.jeurceramsoc.2010.07.004>
- [16] Uematsu, K., Miyashita, M., Kim, J.Y. and Uchida, N. (1992) Direct Study of the Behavior of Flaw-Forming Defect in Sintering. *Journal of the American Ceramic Society*, **75**, 1016-1018. <https://doi.org/10.1111/j.1151-2916.1992.tb04178.x>
- [17] Hondo, T., Kato, Z., Yasuda, K., Wakai, F. and Tanaka, S. (2016) Coarse Pore Evolution in Dry-Pressed Alumina Ceramics during Sintering. *Advanced Powder Technology*, **27**, 1006-1012. <https://doi.org/10.1016/j.apt.2016.04.009>
- [18] Saito, Y., Tanaka, S. and Uchida, N. (2002) CLSM for Ceramic Green Microstructure. *American Ceramic Society Bulletin*, **81**, 35-38.
- [19] Saito, Y., Tanaka, S., Uchida, N. and Uematsu, K. (2001) Direct Evidence for Low-Density Regions in Compacted Spray-Dried Powders. *Journal of the American Ceramic Society*, **84**, 2454-2456. <https://doi.org/10.1111/j.1151-2916.2001.tb01035.x>
- [20] Tanaka, S. (2006) Design of Packing Structures through Direct Characterization of Ceramics Green Bodies. *Journal of the Ceramic Society of Japan*, **114**, 141-146. <https://doi.org/10.2109/jcersj.114.141>
- [21] Tanaka, S., Kato, Z., Uchida, N. and Uematsu, K. (2003) Direct Observation of Aggregates and Agglomerates in Alumina Granules. *Powder Technology*, **129**, 153-155. [https://doi.org/10.1016/S0032-5910\(02\)00226-7](https://doi.org/10.1016/S0032-5910(02)00226-7)
- [22] Kato, Z., Tanaka, S., Uchida, N. and Uematsu, K. (2006) Observation of the Granule Packing Structure Using a Confocal Laser-Scanning Microscope. *Journal of the European Ceramic Society*, **26**, 683-687.

- <https://doi.org/10.1016/j.jeurceramsoc.2005.07.005>
- [23] Tanaka, S., Kuwano, Y. and Uematsu, K. (2007) Packing Structure of Particles in a Green Compact and Its Influence on Sintering Deformation. *Journal of the American Ceramic Society*, **90**, 3717-3719. <https://doi.org/10.1111/j.1551-2916.2007.01975.x>
- [24] Hondo, T., Kato, Z. and Tanaka, S. (2014) Enhancing the Contrast of Low-Density Packing Regions in Images of Ceramic Powder Compacts Using a Contrast Agent for Micro-X-Ray Computed Tomography. *Journal of the Ceramic Society of Japan*, **122**, 574-576. <https://doi.org/10.2109/jcersj2.122.574>
- [25] Deis, T.A. and Lannutti, J.J. (1998) X-Ray Computed Tomography for Evaluation of Density Gradient Formation during the Compaction of Spray-Dried Granules. *Journal of the American Ceramic Society*, **81**, 1237-1247. <https://doi.org/10.1111/j.1151-2916.1998.tb02474.x>
- [26] Cottrino, S., Jorand, Y., Maire, E. and Adrien, J. (2013) Characterization by X-Ray Tomography of Granulated Alumina Powder during *in Situ* Die Compaction. *Materials Characterization*, **81**, 111-123. <https://doi.org/10.1016/j.matchar.2013.04.004>
- [27] Lu, P., Lannutti, J.J., Klobes, P. and Meyer, K. (2000) X-Ray Computed Tomography and Mercury Porosimetry for Evaluation of Density Evolution and Porosity Distribution. *Journal of the American Ceramic Society*, **83**, 518-522. <https://doi.org/10.1111/j.1151-2916.2000.tb01227.x>
- [28] Ku, N. (2015) Evaluation of the Behavior of Ceramic Powders under Mechanical Vibration and Its Effect on the Mechanics of Auto-Granulation. Ph.D. Thesis, Rutgers University, New Brunswick.
- [29] Alazzawi, M.K., Murali, S. and Haber, R.A. (2017) Visualizing the Effect of Extrusion Velocity on the Spatial Variation of Porosity in a Titanium Dioxide/Binder System. *Materials Sciences and Applications*, **8**, 933. <https://doi.org/10.4236/msa.2017.813068>
- [30] Promdej, C., Areeraksakul, S., Pavarajarn, V., Shigetaka, W., Wasanapiarnpong, T. and Charinpanitkul, T. (2008) Preparation of Translucent Alumina Ceramic Specimen Using Slip Casting Method. *Journal of the Ceramic Society of Japan*, **116**, 409-413. <https://doi.org/10.2109/jcersj2.116.409>
- [31] Yu, B., Feng, Y.J., Wohn, L.S., Huang, C., Li, Y.F. and Jia, Z. (2011) Spray-Drying of Alumina Powder for APS: Effect of Slurry Properties and Drying Conditions upon Particle Size and Morphology of Feedstock. *Bulletin of Materials Science*, **34**, 1653-1661. <https://doi.org/10.1007/s12034-011-0373-0>